Geotechnical Characterization of Kangra Valley Landslide

Swati Sharma* and A.K. Mahajan*

Abstract

This study presents the numerical simulation of slopes through the stability analysis of a major landslide which occurred on 14 August 2013 after a prolonged rainfall episode and affected the Tiralines village near Dharamshala city of district Kangra, Himachal Pradesh. The study involves the field investigations, a geotechnical study of the slope material's index properties and numerical modelling using 2D finite element method (FEM) for finding the cause and nature of the landslide. Three slope models have been used for the stability analysis in Phase[2] software. An external building load/force is applied in model 1 of the slope section 'A' whereas, for model 2 of the slope section 'A' no external building load was used. Model 3 for section 'B' is from the same landslide body representing the natural slope exposed after the first landslide episode. All the models were simulated for the critical strength reduction factor (SRF) beyond which the slope would fail. The results reveal a low critical SRF value 0.85 for model 1 at which the maximum displacement of 0.22 m was computed for the lower portion of the slope section 'A' which looks vulnerable. The SRF value 1.27 for model 2 and 1.15 for model 3 shows comparative marginal stability theoretically but, the field conditions indicate critical slope nature.

Keywords: Landslide; Characterization; Kangra; FEM

Introduction

Landslide is one of the main natural hazards leading to global economic as well as societal loss and this phenomenon has alone affected almost 15 per cent of the Indian landmass (Onagh et al., 2012) out of which maximum landslide events are restricted to the Himalayan region especially in the north and north-eastern parts. Many parts of

* **Swati Sharma** and **A.K. Mahajan**, Department of Environment Science, School of Earth and Environmental Sciences, Central University of Himachal Pradesh, India. Corresponding Author Email: swati.9238@gmail.com, Email: akmahajan@rediffmail.com

the Himalayan region generally remain under stress due to the continuous northward movement of the Indian landmass causing dynamic tectonic activities (Sharma and Mahajan, 2018) leading to earthquakes, mass movements, subsidence, etc. The developmental activity in the Himalayan regions can only be accomplished with proper geological and geotechnical studies on large scale for safer constructions (Fall et al., 2006) however, most of the road and the settlements are worst hit due to landslide movements reflecting poor planning and applications of unscientific methods for planning constructions (Anabalgan et al., 2008). Natural slope stability in hilly regions is usually distorted due to the unplanned excavations for new constructions or widening of transportation routes, extreme climatic conditions such as a prolonged rainfall event or an earthquake in areas with structural discontinuities, vegetation patterns that slowly degrade the quality of slope material, etc. (Anabalgan et al., 2008), (Singh et al., 2014) and (Umrao et al., 2011). Considering the number of challenges faced by the Himalayan slopes, the stabilization process requires slope stability analysis and use of engineering applications. The stability of rock slopes or the debris slope depends on the inherent properties of the material (porosity, permeability, type of material, plasticity, shear strength) and the internal and external forces that are exerted on the slopes (Singh et al., 2016).

The detailed slope stability analysis for a landslide is categorised under the post-disaster evaluation of various geotechnical parameters and using them as input for simulating the actual slope conditions in computer-based programmes. Number of such stability analysis methods (limit equilibrium method) proposed by Janbu (Janbu, 1968), Bishop (Bisho, 1995), Morgenstern (Morgenstern and Price, 1965) and Spencer (Spencer, 1967) have been widely used which involve number of assumptions along with the problems of dealing with slope material heterogeneity and the varying slope geometry. In contrast to the limit equilibrium method, the numerical modelling approach like Finite Element Method (FEM) considers the slope material's homogeneity and inter-slice force determination for giving the factor of safety value for slopes (Kanungo et al., 2013) therefore, it is more efficient and preferred method due to its non-linear nature and ease of simulating the heterogeneous slope material and has been used by various researchers (Savage et al., 2000; Quecedo et al., 2004; Singh and Verma, 2007; Sarkar and Singh, 2007; Sarkar et al., 2012; Singh et al., 2013; Kanungo et al., 2013; Singh et al., 2013; Verma et al., 2013; Mahanta et al., 2016; Singh et al., 2016; Gupta et al., 2016 and Jamir et al., 2017). FEM is therefore much useful and now is coupled with the shear strength reduction method (Matsui and San, 1992) using the criteria of reducing the shear strength of the material (successive reduction of cohesion(c) and friction angle (φ) by a certain factor called shear strength reduction factor (SRF) as shown in Eqs. (1) and (2) till the slope failure occurs which is considered as the value of factor of safety (FoS) for the slopes.

$$c_f = \frac{c}{SRF} \tag{1}$$

where, c_f is the reduced cohesion factor

$$\Phi_f = \frac{\Phi}{SRF} \tag{2}$$

where, Φ_f is the reduced friction angle factor

In this study, 2D Finite Element Method (FEM) has been utilised for modelling the debris slopes of a major landslide in Tirah village near to Dharamshala town, Himachal Pradesh, India. The geotechnical properties of the slope material, the field studies and the previous literature data have been used as input in FEM modelling with the help of computer-based Phase^2 software (Rocscience, 2010) for the numerical simulations. Kanungo et al. (2013) described the failure criteria most suitable in FEM based studies i.e. non-convergence of solution within the user-specified iterations at a point of simultaneous slope failure and a similar approach was followed in this study. The landslide area under consideration is sandwiched between the major Thrusts namely Main Boundary Thrust (MBT) in the north and a local Drini Thrust/Murree Thrust in the south, making it tectonically very active (Mahajan and Kumar, 1994). This study highlighted the critical zones on the landslide site which have the highest stress accumulations that should be subjected to mitigation and continuous monitoring.

Study Area and Field Observations

The Tiralines landslide is located on Dharamshala-Mcleodganj road (32°13’ N-76°19’ E), almost 2.5 km from the main Dharamshala city in the district Kangra of Himachal Pradesh (Fig. 11.1). The general elevation of the Tiralines landslide is 1600 m a.m.s.l and fall on a survey of India toposheet number 52D/8. This landslide event occurred in the month of August 2013 situated in the Dharamshala cantonment which comes under wet-temperate zone with annual precipitation of 2900 ± 639 mm and the mean annual temperature of 19°C.

Fig. 11.1: Location of the study area

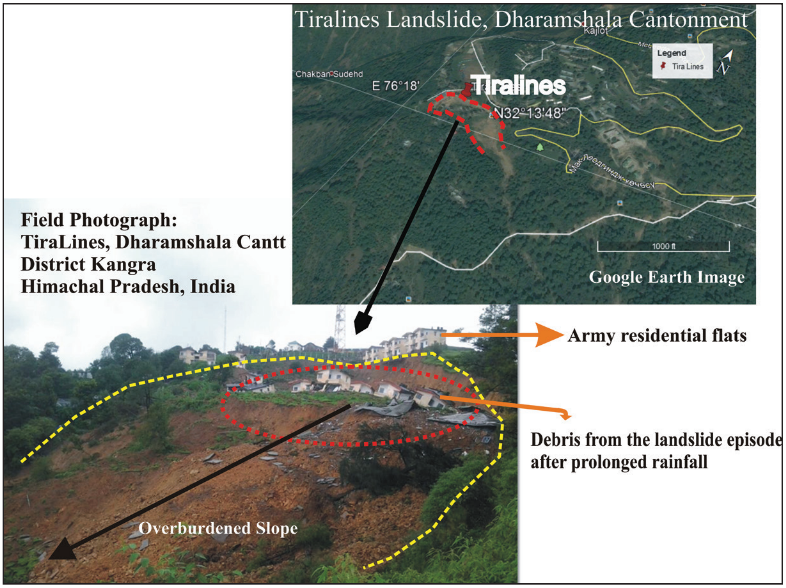

The Tiralines landslide is one of its kinds in this region as it destroyed almost 28 local and army residences after continuous downpour for 4 days in August 2013. The landslide affected area is mainly covered by debris and chunks of weathered rock material from the surrounding slopes. The landslide zone is underlain by Dharamsala Group of rocks constituting sandstones with alternating clays, shale and siltstone bands forming part of the Outer Himalayan zone. The sandstone is highly Feldspathic in nature and thus is highly moisture absorbing. Since the Dharamsala Group of rocks comprises three different lithology i.e. sandstone, claystone and siltstone; the impermeable claystone layer which is overlain by the debris material easily absorbs moisture during the precipitation events and provides an easy sliding plane leading to slope instability. The alternating sandstone, claystone and siltstone layers are highly weathered in the study area (Fig. 11.2). The detailed contour map of the landslide was prepared based on the total station survey method at the scale of 1:500 with 1m contour interval (Fig. 11.3) which shows the morphology of the landslide body. The landslide site was investigated for studying the various slope sections, type of mass movement and for the sample collections.

The Tiralines landslide is a potential debris slide and is situated less than 150 m away from the main road connecting the army cantonment area with other parts of the Dharamshala city. Towards the crown area of the landslide body are the buildings of army settlement few of which were badly destroyed because of the landslide event. The total affected area of landslide as mapped is 19062 m^2 which affected the nearby slopes and has increased the chances of future slope failure in its vicinity. The general slope angle of this landslide varies between 40° to 45° and the slope orientations vary between N 105° and N 145°. The landslide is located in the Dharamsala Group of rocks which has sandstone as the bedrock seen to be exposed in a small patch near to the landslide area and is highly weathered. The slopes have debris cover of almost 20 to 25 m which has been estimated based on field observations and also the bedrock was exposed somewhere 25 m south to the crown part of the landslide near the lateral side of local drainage. The overlying debris material on the slopes seems to be a product of weathering of the bedrock (sandstone) as it has sandy cobbles and pebbles which are very fragile and other parts of the debris material are the Quaternary glacial deposits. Numbers of lateral cracks were observed during the field studies which must have played an important role in the sliding event as the damage occurred after a prolonged rainfall episode and the cracks or the fissures remain the easiest path for water to percolate sub-surface.

Fig. 11.2: View of the Tiralines landslide from August 2013 showing amount of damage and the latest view of the area showing the settlements just above the damaged slope

Methodology

Field investigations were carried out at 1:500 scale as shown in Fig. 11.3, to study the type of the slope material movement. The arbitrary latitude-longitude and the corresponding elevation values were recorded using the total station method (Table 11.1) which resulted in the detailed map of the landslide site that was geo-referenced using the global positioning system (GPS) points recorded during the field survey. The landslide falls under army jurisdiction where any kind of scientific drilling was not permissible. The landslide site was then investigated for studying the various slope sections, type of mass movement and sample collections. From the landslide body, two slope sections (sections A and B) were chosen for the slope stability analysis. The choice of these slope sections was based on their potential steepness and elevations which create the possibility of future landslide episode under similar physical/ climatic conditions that triggered the slope failure under study. The collection of the representative samples from the landslide body was performed in order to find out their index properties for using in the computer-based finite element modelling in the Phase^2 (version 6.0) software.

Table 11.1: showing total station survey readings (Latitude-Longitude and Elevations) for detailed mapping of the Tiralines landslide

Arbitrary Latitude	Arbitrary Longitude	Elevation (m)
1000	2000	500
1007	2000	501.2
1009.004	1993	504.259
1021.33	1983.154	509.578
1027.189	1927.32	507.941
1001.963	1911.401	505.443
979.573	1904.249	505.293
961.436	1916.742	498.591
962.93	1921.122	494.602
975.042	1917.953	496.57
994.05	1926.081	496.503
1005.615	1951.497	491.332
994.398	1980.091	488.946
986	2009.527	488.248
963.325	2044.356	479.308
948.611	2028.695	482.937
944.226	2004.988	484.376
951.486	1995.523	487.399
970.809	1971.089	487.586
976.772	1948.947	489.939
982.352	1939.822	493.517
966.142	2014.691	486.701
948.052	1923.921	492.547

937.319	1952.91	486.744
991.568	2015.082	496.146
922.426	2084.847	490.472
936.384	2017.663	477.383
915.006	2017.806	470.759
907.96	1971.776	472.115
883.258	1985.456	461.878
894.967	2017.387	462.045
904.312	2052.778	460.683
881.545	2066.115	456.482
869.003	2050.718	449.944
862.147	2030.312	451.178
838.582	2023.289	448.832
822.193	2046.137	444.081
796.565	2076.796	428.666
811.822	2085.398	431.964
832.116	2067.076	438.489

Fig. 11.3: Contour Map of the study area at a scale of 1:500 & 1m contour interval (inset slope sections A and B for the stability analysis)

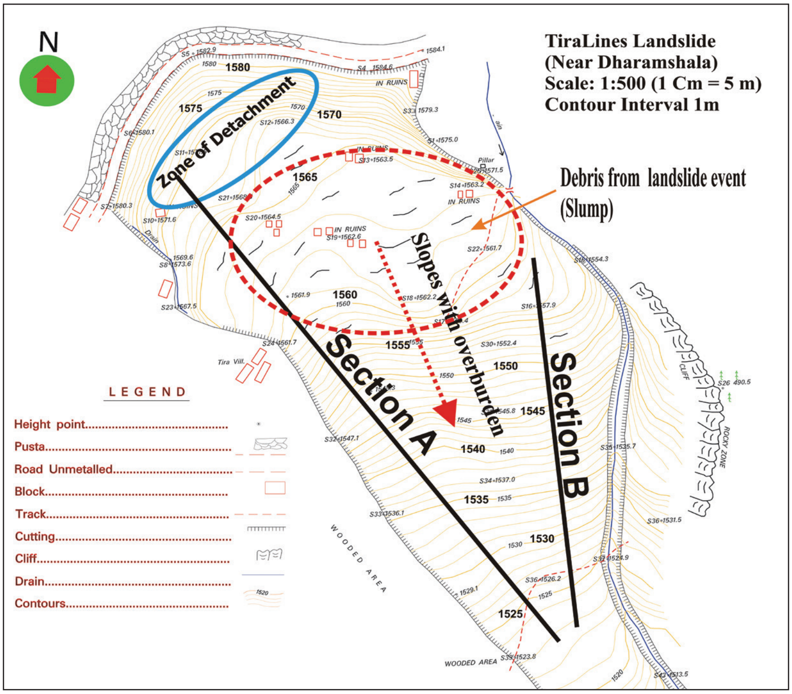

The soil samples representing the actual slope material were collected from different parts of this landslide body from a depth of almost 1 m beneath the surface: sample I from the area near the zone of detachment (top), sample II from the area near to the middle of the landslide body and sample III from the area near to the toe of the landslide body (bottom). These representative soil samples were stored in the air tight plastic bags and were transported to the laboratory for determining their geotechnical properties (as per standard procedures) such as grain size distribution, dry density (gm/cm^3), liquid limit (per cent), plastic limit (per cent), permeability (cm/sec), cohesion (kPa) and friction angle (°). Also, the field density (gm/cm^3) of slope material was determined at the sites of the sample collection. Two slope sections A and B were chosen from the detailed map of the landslide (Fig. 11.3) to prepare the slope models representing their geometry and vulnerability towards the future sliding event. The slope sections of the landslide for using in the slope modelling were extracted from the ASTERGDEM data of 30 m resolution (obtained from USGS website https://earthexplorer.usgs.gov/). The determined material properties from the geotechnical lab studies were incorporated in the numerical simulations carried out with help of 2D finite element method (FEM) for the chosen slope sections.

Geotechnical Properties of Slope Material

Geotechnical properties of the slope material evaluated for the study are Grain size analysis, field density, dry density, optimum moisture content, liquid limit, plastic limit, specific gravity, permeability, cohesion and the friction angle.

Grain size analysis (Sieve method) and soil consistency

This test determines the per cent distribution of various grain sizes (coarse, medium and fine grain) in the soil samples. The soil sample collected was sun-dried, sieved and the grain size analysis was carried out as per BIS (1985) IS 2720 (Part 4). Fig. 11.4 represents the grain size distribution curves for the analyzed soil samples according to which they were classified.

The soil consistency indicates the firmness of the soil and its behaviour at various water contents (Koner and Chakravarty, 2016) which is represented as the Atterberg limits of the soil. Table 3 shows the values of LL, LP and Ip derived as per Indian Standard {BIS (1985) IS 2720 (Part 5)} and indicated maximum plasticity in sample 2 (Ip = 14.6%) whereas sample 1 indicates least plasticity (Ip = 2.2 per cent).

Overall the analysed soil samples reflected the majority of sandy composition i.e.

76.5 per cent to 82.4 per cent followed by the silt and clay mixture varying from 9.5 per cent to 12.1 per cent and lastly the gravels ranging between 8.1 per cent to 11.4 per cent. As shown in Table 11.2, sample-1 with 11.4 per cent gravels, 76.5 per cent sand and 12.1 per cent silt + clay mixture is classified under silty sand (SM) category as per unified classification method {BIS (1970) IS 1498}. Following the similar soil classification method for sample-2 (82.4 per cent sand, 8.1 per cent gravel and 9.5 per cent silt + clay mixture) and sample-3 (79.5 per cent sand, 10.2 gravel and 10.3 per cent silt clay mixture) were classified as SW-SM (well-graded sand to silty sand) and SP-SM (poorly graded sand to silty sand) respectively.

Table 11.2: Grain size distribution and classification of the soil samples

Grain Size Analysis	**Sample 1**	**Sample 2**	**Sample 3**
Composition	Gravel 11.4% Sand 76.5% Silt + Clay 12.1%	Gravel 8.1% Sand 82.4% Silt + Clay 9.5%	Gravel 10.2% Sand 79.5% Silt + Clay 10.3%
Cu (coefficient of uniformity)	11.11	14.44	14.29
Cc (coefficient of curvature)	1.78	1.37	0.89
Soil Classification (Unified System) As per IS 1498	SM (Silty Sand)	SW-SM (Well graded sand to Silty Sand)	SP-SM (Poorly Graded Sand to silty sand)

Table 11.3: Atterberg limits of the soil samples

	Liquid Limit (%)	**Plastic Limit (%)**	**Plasticity Index (%)**
Sample 1	22.9	20.7	2.2
Sample 2	23.1	8.5	14.6
Sample 3	19.5	15.3	4.2

Fig. 11.4 Grain-size distribution curves of sample 1 (top), sample 2 (middle) and sample 3 (bottom)

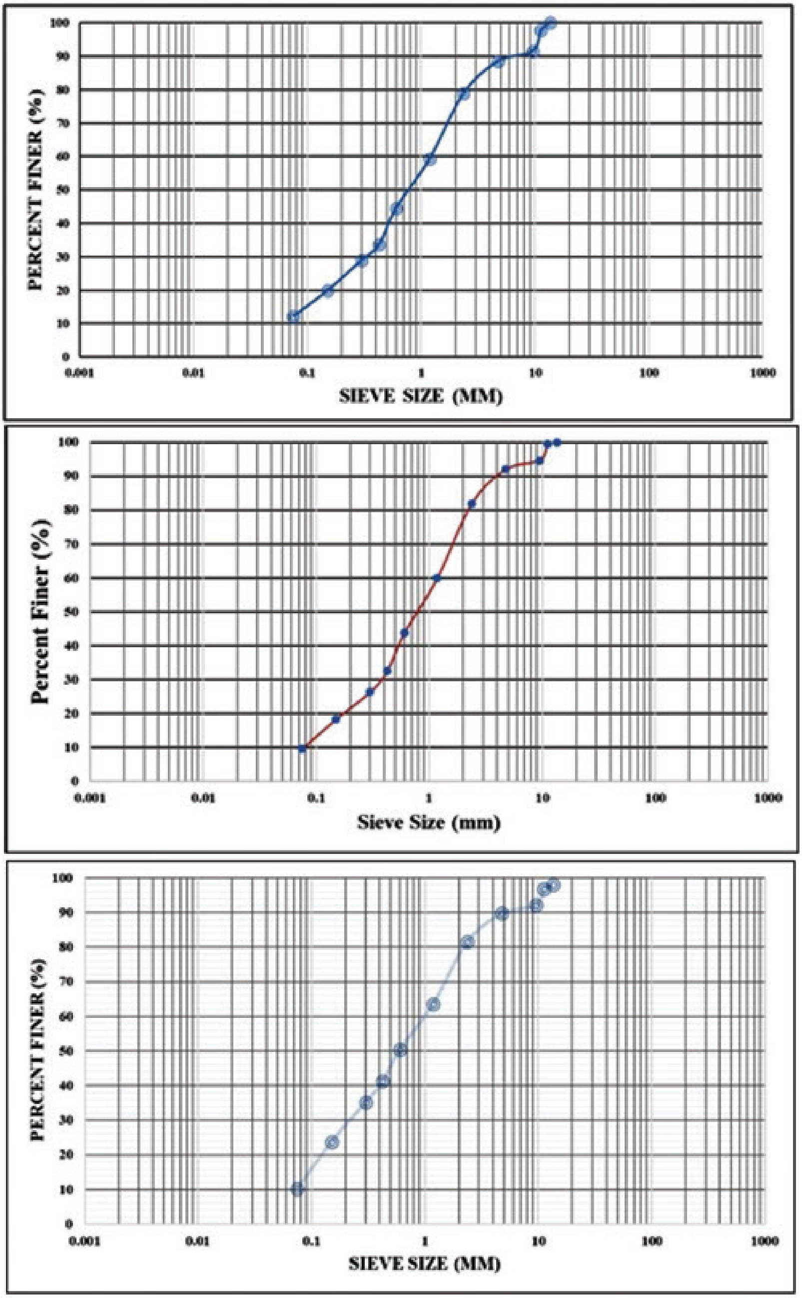

Permeability (K) and optimum moisture content (OMC) of the soil samples

In this study as all the soil samples were medium to fine-grained therefore falling head permeability test method was used to check their hydraulic conductivity as per Indian Standard {BIS (1986) IS 2720 (Part 17)}. The permeability (K) was measured as per the Eq. (3):

$$K = \frac{2.3\,al}{A(t_1 - t_0)} \log_{10} \frac{h_0}{h_1} \quad (3)$$

Where, K is the permeability, a is the cross-sectional of area vertical cylinder, l is the length of a cylinder which is connected to a stand pipe of cross-sectional area A, the water level is set at a height h_0 at time t_0, when the water starts draining into the sample water level falls at h_1 at time t_1 the water head drop was measured as $h_0 - h_1$ whereas, the time elapsed to drop the water head was noted as $t_1 - t_0$.

Table 11.4 shows the permeability range of the samples analysed from the study area which varies from 4×10^{-5} cm/sec to 4.66×10^{-5} cm/sec.

The field density (in-situ) of the soil samples were determined based on Indian standard {BIS (1975) IS 2720 (Part 29) and Table 11.4 shows the field density (gm/cm^3) of the tested samples. The dry density of the soil samples and the optimum moisture contents (OMC) were determined using modified proctor compaction methods as per Indian Standard {BIS (1983) IS 2720 (Part 8)}. The bulk density of the soil sample (γ) is calculated as per the Eq. (4):

$$\gamma = \frac{(W2-W1)}{V} \ \text{gm/cm}^3 \quad (4)$$

W_1 & W_2 are the weights of a sample, (W) is the moisture content, V is the volume of the cylindrical mould

The dry density γ_d was calculated as per Eq. (5):

$$\gamma_d = \frac{100\,\gamma}{(100+W)} \ \text{gm/cm}^3 \quad (5)$$

where, W is the moisture content and γ is the bulk density of the soil samples

Number of such determinations of dry density and moisture content were made and plotted on a graph where, the peak point on the graph corresponds to the optimum moisture content (OMC) of the soil samples. Table 11.4 shows the values of dry density and the OMC of the soil samples analysed.

Table 11.4: Geotechnical properties of the representative soil samples from the Tiralines landslide

Material Properties	Field Density(gm/cm³)	Dry Density (gm/cm³)	OMC (%)	Permeability (cm/sec)	Cohesion (kPa)	Friction Angle (°)
Sample I	1.24	1.35	17.5	4.66×10^{-5}	0.07	25
Sample II	1.66	1.76	15.3	4.66×10^{-5}	0.02	27
Sample III	1.8	1.83	15.4	4×10^{-5}	0.17	31

Shear strength parameters

The shear strength of the soil is considered as the strength of sample to resist change till the point of failure. To derive the shear strength parameters, which are cohesion (c) and friction angle (Φ) direct shear test method was performed as per Indian Standard {BIS (1986) IS 2720 (part 13)}. The soil samples were prepared in a shear box of 6 cm × 6 cm dimension in a remolded form. The resulting values of cohesion and friction angle for the analysed samples are shown in Table 11.4.

4 Numerical simulations using finite element method (FEM)

Fig. 11.5: Slope section A and B extracted from the DEM data for using in the finite element modelling phase showing the slope geometry

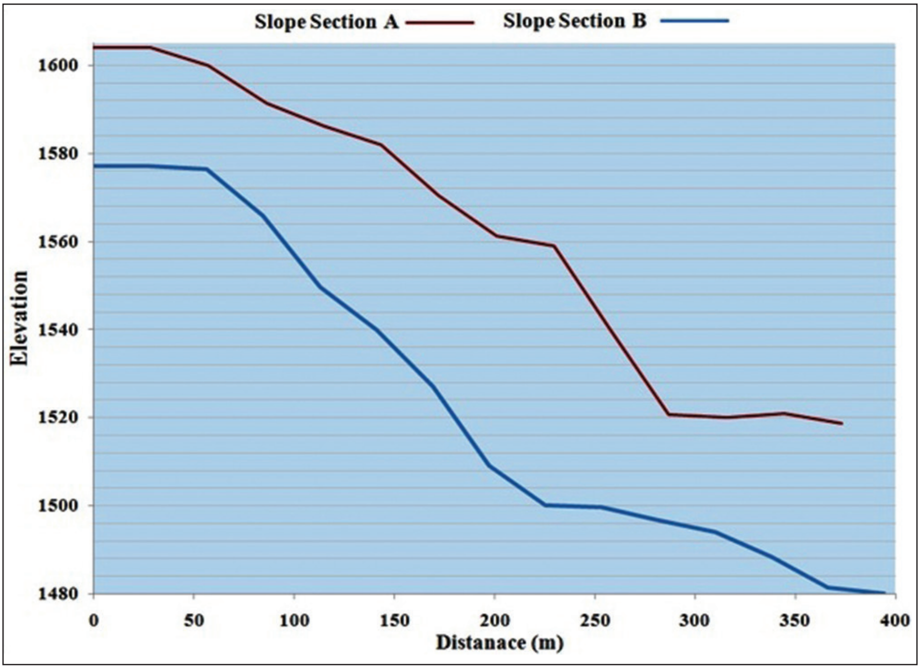

In this study Phase2 software was used for FEM based continuum analysis for which the slope section A and B on the landslide zone were marked (Fig. 11.5) with the help of 30 m resolution digital elevation model DEM. First, the slope sections were imported into the Phase^2 software for finite element analysis and then were discretised into a finite number of domains (Fig. 11.6) without any set dimensions or pre-assumption of the slip surface shape or depth (Jing, 2013). The slope section domains are connected to each other with nodes and the forces are applied on these nodes which cause various interactions while the modelling. This modelling method records the strength reduction factor (SRF) values for the slope material at progressive strength reduction (SSR) (reduced cohesion 'c' and friction angle ϕ until the failure occurred Three slope models (Fig. 11.6) were used for stability analysis out of which for the slope section A, two types of scenarios were studied: slope model 1 with external building load and slope model 2 without external building load. The slope model 3 was analysed for section B on the landslide body which was without any external load and represented a separate lower portion on the landslide body vulnerable to sliding because of its observed geometry and overburden from the previous sliding (August 2013) in section A. All the slope models represented heterogeneous material i.e. overlying debris material on slopes and the basement rock i.e. sandstone. The material properties of the sandstone were taken as the standard value (Marinos and Hoek, 2000) and (Cai et al., 2004) as drilling was not performed to collect the core sample till the basement rock. For the overlying soil cover, lab investigations of the geotechnical properties and standard values for elastic modulus and Poisson's ratio by Gercek (Gercek, 2007) and Hoek et al. (Hoek et al., 2002) were used. This analysis involves the use of Mohr-Coulomb failure criteria (Janbu, 1968) for upper debris soil material and Hoek-Brown generalized criteria for the basement rock (sandstone) (Table 11.5). The slope was discretised into uniform mesh of two dimensional- 6 nodded triangular elements in three of the slope models. For slope model 1 and 2 overall 1974 elements were created to mesh the slope which has 4101 nodes and the mesh quality was ensured as only 23 mesh elements out of 1974 were of low quality which is only 1.2 per cent of the total elements. The slope model 3 (slope section B) was meshed with 1375 elements connected with 2902 nodes and only 1.1 per cent elements of low quality. The boundary conditions of the slope models were fixed (no displacements) on lateral sides and the bottom of the slope models, whereas kept free for the upper slope surface. The slope models were then subjected to loading i.e. only the body force (gravity load) in case of model 2 and model 3 whereas, gravity loading along with the vertical stress (external uniform building load) were applied for model 1. All the material properties were incorporated appropriately for the slope materials (overburden debris soil and sandstone) and the finite element modelling was run for shear strength reduction of the material till the critical strength reduction factor (SRF) was achieved.

Fig. 11.6 Finite element models 1 & 2 for slope section A of Tiralines landslide (model 1 with building load and model 2 without external load), model 3 for section B used in Phase2 software

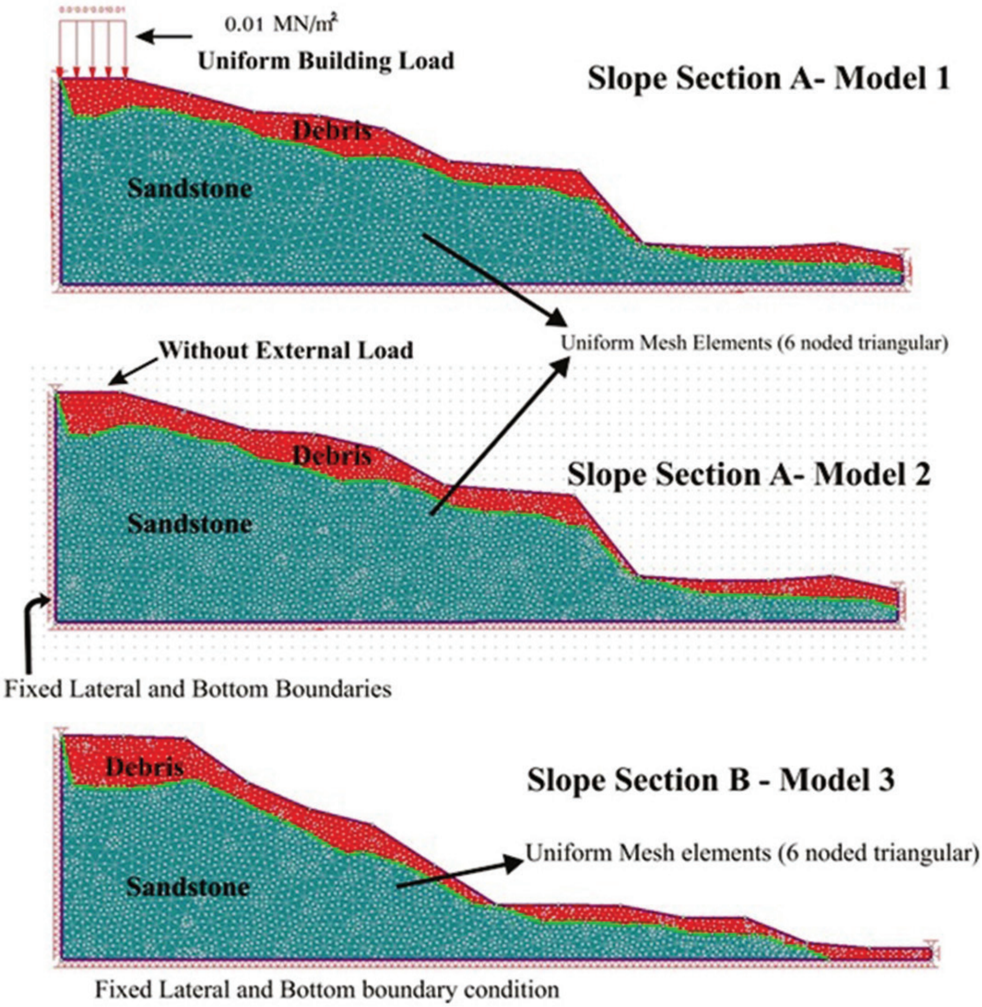

Table 11.5: Failure criteria for various slope materials and their properties used in finite element (FEM) continuum modelling, Kanungo et al. (Quecedo et al., 2004)

S. No.	Material	Model
1.	Overburden (Debris)	**Mohr-Coulomb,** (Gercek, 2007) $\tau = c + \sigma tan\varphi$ Where, τ is the shear strength of slope material, c and Φ are the shear strength parameters Initial element loading = Field stress and Body force Dilation Angle = 0 (natural slope), Hoek et al. 2002 Unit weight = 0.0205 MN/m^3, Poisson's ratio (υ) = 0.28, Young's Modulus = 20 MPa, Elastic type = isotropic
2.	Sandstone	**Generalized Hoek & Brown,** Marinos and Hoek, 2000 and Cai et al., 2004 $\sigma_1 = \sigma_3 + \sigma_{ct}\left[m_b\frac{\sigma_3}{\sigma_{ct}} + s\right]a$ σ represents the principal stresses, Where, m_b is the reduced value of the material constant m_i, Constant s and a, depend on the property of the rock type. Dilation Parameter = 0 (natural slope) Element Loading = Field stress and Body force Unit weight = 0.027MN/m^3, Poisson's ratio = 0.3, Young's Modulus = 20,000 MPa, Elastic type = isotropic, GSI = 50 MPa, a = 0.5, s = 0.0001, mb = 0.3

Results and Discussion

For discretised and meshed slope models 1, 2 and 3 (Fig. 11.6) shear strength reduction (SSR) analysis was carried out using Phase² software, in which the stresses were applied on each uniform mesh element. This finite element modelling (FEM) determined the critical strength reduction factor (SRF) values using plain strain analysis for each slope model and the maximum displacement of slope material at that critical SRF values (Fig. 11.7). The numerical simulation results (Table 11.6) for model-1 of slope Section-A reflected critical SRF value of 0.84 with a maximum displacement of 0.35 m at this SRF.

For slope model-2 of Section-A without external loading, the critical SRF value 1.27 with a maximum displacement of 0.2 m resulted. Model-3 for the slope Section-B has shown a critical SRF value 1.15 with maximum displacement value of 0.84 m. The Section-B had much steeper slope from the middle to lower parts whereas, the crown area seems to be in stable condition because of its geometry which resulted in marginal stability value of 1.15. The results for the slope Section-A of the Tiralines landslide with building load (model-1) resulted into SRF value 0.84 which reflected its unstable condition. This clearly indicates that the slope material had low shear strength to bear the load of multistoried settlements and the added impact of the prolonged rainfall event in August 2013 led to the massive mass movement that destroyed many houses. Obviously, with the previous settlements on this weak slope, the domestic drainage and the sewerage system were also unscientifically constructed and the water kept seeping through this weak slope material and led to the ultimate slope failure.

Table 11.6: Results of the FEM based modelling for slope Sections A and B

S. No.	Strength Reduction Factor (SRF)	Maximum Shear Strain	Maximum Displacement (m)
Model 1 (Section A)	0.84	0.19	0.35
Model 2 (Section A)	1.27	0.07	0.20
Model 3 (Section B)	1.15	0.10	0.84

The slope model-2 for section-A of the landslide shows SRF value 1.27 which indicates the marginal slope stability as reflected in Fig. 11.7, the steep downhill side of the slope shows maximum displacement of material. The uphill side of slope section A is mainly covered with debris from the previous landslide also but the lower side of the slope being steeper can fail due to overburden pressure. Maximum displacement for slope models 1 and 2 is indicated at the lower parts of the slope, highlighted with the bright critical zone (Fig. 11.7).

Fig. 11.7: Shear strength reduction (SSR) results for slope models showing the critical SRF values

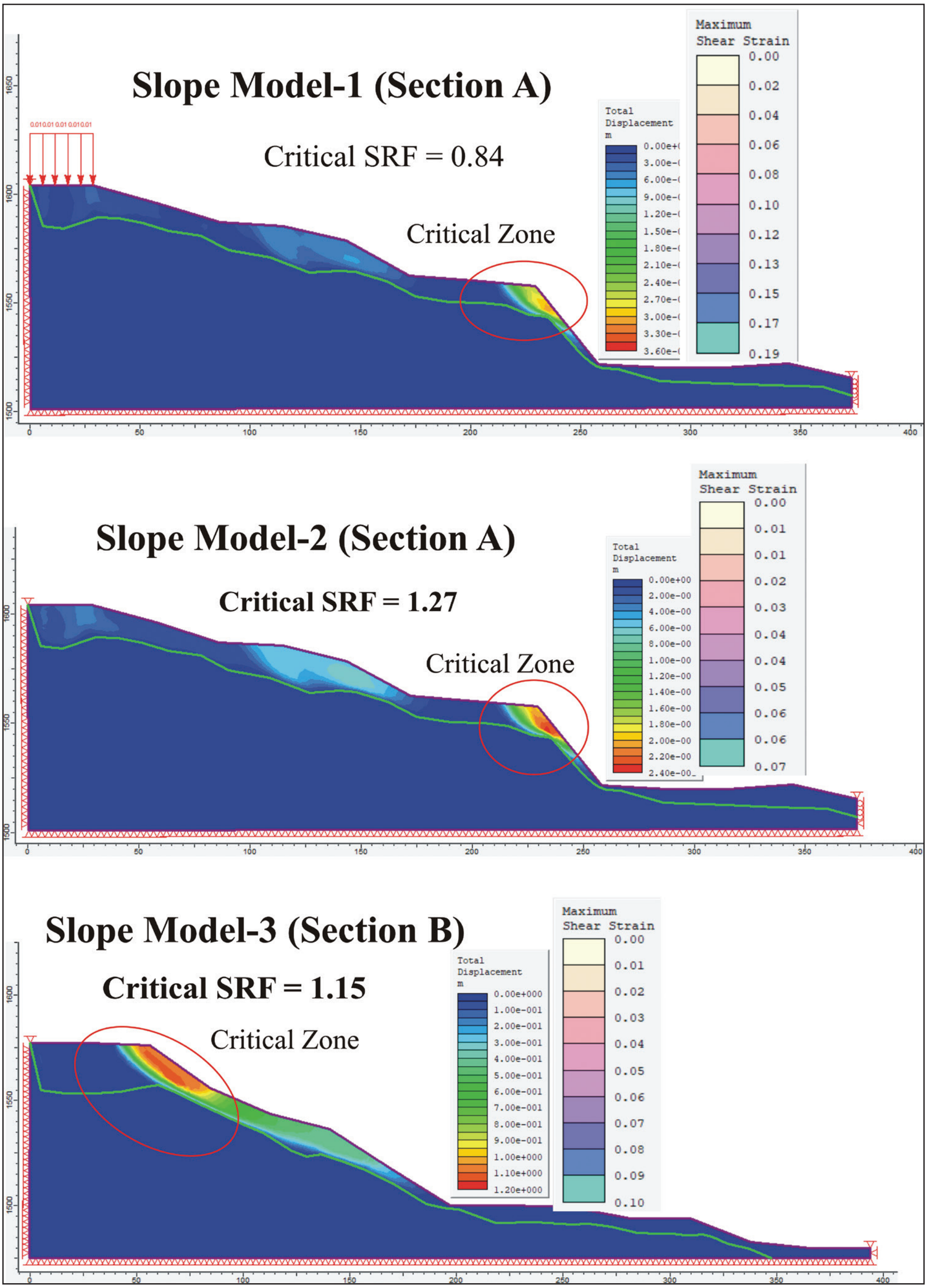

The maximum shear strain value for the slope model-1 is highest showing an agreement with its low value of critical strength reduction factor (SRF) 0.84. The results show agreement with the field conditions accurately as while the field studies the critical slope behaviour was much obvious with the observation of lateral cracks, water seepage from nearby seasonal drainage and tilting of shrubs on the slopes. Therefore, keeping in view the critical zones on the slope sections of models 1, 2 and 3 instrumentation for monitoring the future landslide activities and mitigation of present problems can be suggested. This landslide site is very sensitive as the debris from the first mass movement in 2013 were cleared off towards the toe area of the hill slope which has increased the overburden pressure and this can lead to another sliding episode in future.

This study on the detailed scale (1:500) for the Tiralines landslide near the Dharamshala city has helped in representing the slope problems and the local causal factors leading to the destruction of infrastructure or transportation routes in such a developing area. The study has revealed the geotechnical properties of the slope material in detail indicating the sandy composition of the overlying slope material which reflects the coarser grain size with small amount of fines (clay + silt) that can allow higher permeability of water into the slope and thus increasing the pore pressure leading to the slope instabilities.

The samples analysed in this study have shown low liquid and plastic limit values for the soil with sandy and lesser fines classification. This mainly indicates the phenomenon that led to the easy water percolation into the slope sub-surface mainly composed of weathered by-products of the sandstone i.e. poorly to well-graded sandy plus silty soil. The dry density values increased for the sample collected from the crown (sample I), middle parts (sample II) and the toe region (sample III) of the landslide body respectively which revealed that the slope material from the upper parts was less compact with more void ratio (higher moisture content) whereas the soil from the middle and toe portions were more compacted with higher dry density and lesser void ratio. The coefficient of permeability values calculated for the soil samples in this study ranged between 4 and 4.66×10^{-5} cm/sec which indicated the presence of sand with gravelly compositions and little amount of fines which was also proportionate with the analysed grain size values. All these results from the geotechnical investigations revealed that the nature of the slope material from the study area could not bear the increased pore pressure due to the prolonged rainfall episode along with the added load of the multi-storey buildings on it. This primarily indicated the nature of slopes from the overall Dharamshala region with debris soil materials overlying the basement rocks, which will not remain stable due to heavy rainfall, unplanned installation of the sewerage systems or the water reservoirs in this hilly terrain. Therefore, the overall results from the geotechnical and the FEM based stability analysis study show the marginal to low slope stability at increased soil moisture due to climatic or anthropogenic interference.

Conclusion

The numerical modelling methods for slope stability analysis has evolved as one of the most powerful tools for suggesting mitigation measures post-disaster and can indicate the zones of slope sections that require immediate attention to avoid future landslides. In this study, the finite element method (FEM) was utilized for modelling the debris slopes of Tiralines landslide of near the Dharamshala city of Himachal Pradesh which occurred in the monsoon of 2013 and destroyed many army residential settlements. This study has determined the critical shear strength reduction factor (SRF) and the corresponding maximum displacement values along with the maximum shear strain for the three slope models. The 2D continuum modelling has shown results in agreement with the actual field conditions as the critical zones highlighted on the slope models represent sensitivity towards sliding on the actual ground as well.

- The results have shown the impact of building load on weak slope material in model 1 which has already failed in 2013 Tiralines landslide event. The slope models 2 and 3 indicate marginal stability of the existing slopes because of the overburden pressure from the massive debris of the previous landslide.
- The geotechnical characterization reflected coarse-grained and high permeable nature of the slope material at the landslide site.
- The investigated results from a geotechnical study of the soil from Tiralines landslide can be extrapolated to determine the nature of slope failure of other landslides in its vicinity.

References

Onagh M, Kumra VK, Rai PK (2012) Landslide susceptibility mapping in a part of Uttarkashi district (India) by multiple linear regression method. International Journal of Geology, Œnviron. Earth Sci.2277-2081.

Sharma S, Mahajan AK (2018) Comparative evaluation of GIS-based landslide susceptibility mapping using statistical and heuristic approach for Dharamshala region of Kangra Valley, India. Geoenvironmental Disasters 5(1): 4.

Fall M, Azzam R, Noubactep C (2006) A multi-method approach to study the stability of natural slopes and landslide susceptibility mapping. Eng. Geol. 82:241–263.

Anabalgan R, Chakraborty D, Kohli A (2008) Landslide hazard zonation mapping on meso scale for systematic planning in mountainous terrain. J. Sci. Ind. Res. 67: 486-497.

Singh R, Umrao RK., Singh TN (2014) Stability evaluation of road-cut slopes in the Lesser Himalaya of Uttarakhand, India: conventional and numerical approaches. Bull. Eng. Geol. Environ. 73(3), 845-857.

Umrao RK., Singh R, Ahmad M, Singh TN (2011) Stability analysis of cut slopes using continuous slope mass rating and kinematic analysis in Rudraprayag district, Uttarakhand. GEOMATERIALS 1(03), 79.
Singh TN, Singh R, Singh B, Sharma LK, Singh R, Ansari MK (2016) Investigations and stability analyses of Malin village landslide of Pune district, Maharashtra, India. Nat. Hazards 81(3): 2019-2030.
Fell R,Hartford D (1997) Landslide risk assessment. Paper read at Landslide risk assessment, Proceedings of the international workshop on landslide risk assessment, edited by: Cruden, D. and Fell.
Janbu N (1968) Slope stability computations. Institute for Geotknikk og Fundamenteringslære, Norges Tekniske Høgskole, Soil mechanics and foundation engineering, the Technical University of Norway.
Bishop AW (1955) Use of the slip circle in the stability analysis of earth slopes. GEOTECHNIQUE 5(1):7–17.
Morgenstern NR, Price VE (1965) The analysis of the stability of general slip surfaces.GEOTECHNIQUE15(1): 79-93.
Spencer E (1967) A method of analysis of the stability of embankments assuming parallel inter-slice forces. GEOTECHNIQUE 17(1): 11-26.
Kanungo DP, Pain A, Sharma S (2013) Finite element modelling approach to assess the stability of debris and rock slopes: a case study from the Indian Himalayas. Nat. Hazards 69:1-24.
Savage WZ, Baum RL, Morrissey MM, Arndt BP (2000) Finite-element analysis of the woodway landslide, Washington. U S. Geol. Surv. Bull. 2180: 1–9.
Quecedo M, Pastor M., Herreros MI, Fernández Merodo JA (2004) Numerical modelling of the propagation of fast landslides using the finite element method. Int. J. Numer. Methods Eng. 59(6): 755-794.
Singh TN, Verma AK (2007) Evaluating the slope instability of the Amiya Slide. In 1st Canada-US Rock Mechanics Symposium. American Rock Mechanics Association.
Sarkar K, Singh TN (2007) Evaluation of Instability Analysis of Slope: A Numerical Approach. Min. Eng. 8(10): 11-31.
Sarkar K, Singh TN, Verma AK (2012) A numerical simulation of landslide-prone slope in Himalayan region—a case study. Arabian J. Geosci. 5(1): 73-81.
Singh PK, Wasnik AB, Kainthola A, Sazid M, Singh TN (2013) The stability of road cut cliff face along SH-121: a case study. Nat Hazards 68(2): 497–507.
Singh R, Umrao RK, Singh TN (2013) Stability evaluation of road-cut slopes in the Lesser Himalaya of Uttarakhand, India: conventional and numerical approaches. Bull. Eng. Geol. Environ. 73(3): 845-857.
Verma D, Kainthola A, Gupte SS, Singh N (2013)A Finite Element Approach of Stability Analysis of Internal Dump Slope in Wardha Valley Coal Field, India, Maharashtra. American Journal of Mining and Metallurgy 1(1): 1-6.
Mahanta B, Singh HO, Singh P K, Kainthola A, Singh TN (2016) Stability analysis of potential failure zones along NH-305, India. Nat. Hazards 83(3): 1341-1357.
Gupta V, Bhasin RK, Kaynia AM (2016) Finite element analysis of failed slope by shear strength reduction technique: a case study for Surabhi Resort Landslide, Mussoorie Township, Garhwal Himalaya. Geomat. Nat. Haz. Risk 7(5):1677-1690. DOI: 10.1080/19475705.2015.1102778.
Jamir I, Gupta V, Kumar V, Thong GT (2017) Evaluation of potential surface instability using finite element method in Kharsali Village, Yamuna Valley, Northwest Himalaya. J. Mt. Sci. 14(8): 1666-1676.
Matsui T, San K (1992) Finite element slope stability analysis by shear strength reduction technique. Soils Found. 32: 59–70.
Rocscience (2010) Slide: stability analysis for soil and rock slopes. Rocscience, Toronto.
Mahajan AK, Kumar S (1994) Linear features registered on the Landsat Imagery in the Dharamsala-Palampur area NW Himalaya, vis-à-vis seismic status of the area. Geophysika (2): 15-25.
BIS (1985) IS 2720 (Part 4) – Methods of test for soils, grain size analysis. BIS New Delhi, India.
Koner R, Chakravarty D (2016) Characterisation of overburden dump materials: a case study from the Wardha valley coal field. Bull. Eng. Geol. Environ. 75(3): 1311-1323.
BIS (1985) IS 2720 (Part 5) – Methods of test for soils, determination of liquid and plastic limit of soils. BIS New Delhi, India.
BIS (1970) IS 1498 - Criteria for Soil Classification. BIS New Delhi, India.
BIS (1986) IS 2720 (Part 17) - Indian Standard code of practice for determination of co-efficient of permeability using Falling head permeameter.
BIS New Delhi, India.BIS (1975) IS 2720 (Part 29) Indian Standard code of practice for determination of insitu field density of the soil using core-cutter. BIS New Delhi, India.
BIS (1983) IS 2720 (Part 8) - Method of Test for Soils: Part 8, Determination of Water Content -- Dry Density Relationship using Heavy Compaction. BIS new Delhi, India.
BIS (1986) IS 2720 (part 13) - Indian Standard code of practice for determination angle of shearing resistance and cohesion intercept using Direct Shear Test. BIS New Delhi, India.
Jing L (2003) A review of techniques, advances and outstanding issues in numerical modelling for rock mechanics and rock engineering. Int J Rock Mech Min Sci 40: 283–353.

Marinos P, Hoek E (2000) GSI: a geologically friendly tool for rock mass strength estimation. In: Proceeding of the GeoEng2000 at the international conference on geotechnical and geological engineering. Technomic publishers, Lancaster, Melbourne, 1422–1446.

Cai M, Kaiser PK, Uno H, Tasaka Y, Minami M (2004) Estimation of rock mass deformation modulus and strength of jointed hard rock masses using the GSI system. Int. J. Rock Mech. Min. Sci. 41(1): 3-19.

Gercek H (2007) Poisson's ratio values for rocks. Int. J. Rock Mech. Min. Sci. 44(1): 1-13.

Hoek E, Carranza-Torres C and Corkum, B (2002) Hoek-Brown criterion – 2002 edition. Proc. NARMS-TAC Conference, Toronto, 1: 267-273.